

# Syntheses and characterization of the edge-bridged open metallocenes $M(C_8H_{11})_2$ ( $C_8H_{11}$ = cyclooctadienyl; $M = Ti, V, Cr$ or $Fe$ )<sup>†</sup>

Vichien Kulsomphob,<sup>a</sup> Robert Tomaszewski,<sup>a</sup> Glenn P. A. Yap,<sup>b</sup> Louise M. Liable-Sands,<sup>b</sup> Arnold L. Rheingold<sup>\*b</sup> and Richard D. Ernst<sup>\*a</sup>

<sup>a</sup> Department of Chemistry, University of Utah, 315 S. 1400 E. Rm. DOCK, Salt Lake City, Utah 84112-0850, USA. E-mail: ernst@chemistry.chem.utah.edu

<sup>b</sup> Department of Chemistry, University of Delaware, Newark, Delaware 19716, USA

Received 30th June 1999, Accepted 21st September 1999

The reactions of two equivalents of the cyclooctadienyl anion with various divalent transition metal salts ( $M = Ti, V, Cr$  or  $Fe$ ) led to the formation of the appropriate bis(cyclooctadienyl)metal complexes, isolable as crystalline compounds. Their constitutions have been established through NMR and mass spectroscopies, elemental analyses, and single crystal X-ray diffraction studies. As with the  $M(2,4-C_7H_{11})_2$  and  $M(6,6-dmch)_2$  ( $C_7H_{11}$  = dimethylpentadienyl; dmch = dimethylcyclohexadienyl) complexes, the titanium and vanadium compounds adopt low spin configurations, thereby differing from their metallocene analogs. The structures observed for these complexes in the solid state are similar to those of the  $M(2,4-C_7H_{11})_2$  complexes. The low spin titanium complex also forms a mono(ligand) adduct with CO, although the binding appears noticeably weak due to the steric influence of the edge bridge.

## Introduction

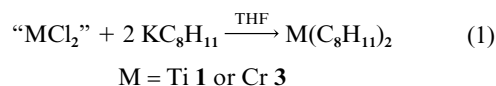
Bis(pentadienyl)metal complexes, or open metallocenes, particularly those containing the 2,4-dimethylpentadienyl (2,4- $C_7H_{11}$ ) ligand, have been demonstrated to possess very significant differences compared to their metallocene counterparts.<sup>1</sup> These differences arise to a large extent from the lower degree of stabilization of the pentadienyl group's occupied  $\pi$  molecular orbitals, and correspondingly greater stabilization of their  $\pi^*$  orbitals, which can lead to greater metal–ligand orbital mixing, stronger metal–ligand bonding, generally higher reactivity, and in some cases low spin configurations.<sup>1,2</sup> While one would expect edge-bridged open metallocenes (“pseudo-metallocenes”<sup>3</sup>), in which the two terminal dienyl carbon atoms are connected *via* a bridging unit, to mimic the unbridged open metallocenes, in some cases these species have been found to possess properties intermediate between those of the metallocenes and open metallocenes (*e.g.*, C–O stretching frequencies of some carbonyl adducts), while in other cases they may even more closely resemble the metallocenes (*e.g.*, green  $Cr(2,4-C_7H_{11})_2$  vs. red  $Cr(C_5H_5)_2$  and  $Cr(6,6-dmch)_2$ , dmch = 6,6-dimethylcyclohexadienyl).<sup>4</sup> In an effort to gain a better understanding of the relationships between pentadienyl, edge-bridged pentadienyl, and cyclopentadienyl ligands, we have investigated the syntheses and natures of bis(cyclooctadienyl) complexes of titanium, vanadium, and iron, as well as for the previously reported chromium complex. It will be seen that the  $C_8H_{11}$  ligand appears to bear greater similarity to the 2,4- $C_7H_{11}$  rather than the 6,6-dmch ligand.

## Results and discussion

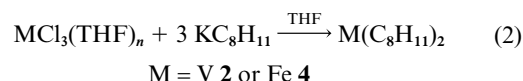
### Synthetic and spectroscopic

The reactions of divalent metal halide complexes of titanium or chromium with two equivalents of  $K(C_8H_{11})$  ( $C_8H_{11}$  = cyclo-

octadienyl) lead to the respective  $M(C_8H_{11})_2$  complexes, eqn. (1). Similarly, the reactions of  $VCl_3(THF)_3$  or  $FeCl_3$  with



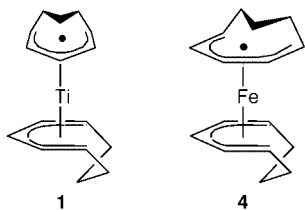
three equivalents of  $K(C_8H_{11})$  lead to analogous vanadium and iron complexes, eqn. (2), thereby demonstrating the ability of



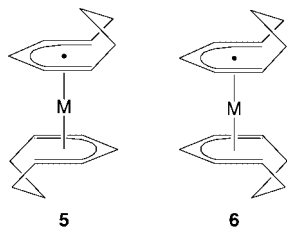
the cyclooctadienyl anion to serve as a reducing agent, as is typical of pentadienyl anions in general. The chromium complex **3** had been reported earlier,<sup>5</sup> but prepared through a different route, as also had been the ruthenium analog.<sup>6</sup> Complexes **1–3** are similar to their  $M(2,4-C_7H_{11})_2$  counterparts in being deep green, while **4** resembles  $Fe(2,4-C_7H_{11})_2$  in being orange-red.<sup>7</sup> All of these complexes are solids (*cf.*, liquid  $Ti(2,4-C_7H_{11})_2$ ), and crystallize much more readily than their  $M(2,4-C_7H_{11})_2$  analogs. As a result, the edge-bridged complexes may well prove to be superior to the  $M(2,4-C_7H_{11})_2$  complexes in various applications such as metal film depositions,<sup>8</sup> naked metal reactions,<sup>9</sup> syntheses of new materials,<sup>10</sup> and polymerizations.<sup>11</sup> The iron complex is relatively air stable, unlike the earlier metal species, and **1** is even pyrophoric on occasion.

In addition to analytical and mass spectral data, NMR spectroscopy proved valuable for the characterization of some of these species. As was found for the  $M(2,4-C_7H_{11})_2$ <sup>1</sup> and  $M(6,6-dmch)_2$ <sup>4</sup> complexes, the 14 electron  $Ti(C_8H_{11})_2$  **1** and 18 electron  $Fe(C_8H_{11})_2$  **4** species are diamagnetic, whereas 14 electron titanocenes are paramagnetic.<sup>12</sup> The NMR spectra of both **1** and **4** reveal unsymmetric ground state conformations, presumed to be as shown below, based upon observations for the  $M(2,4-C_7H_{11})_2$  complexes. At higher temperatures, one observes the establishment of a more symmetric NMR pattern for **4**, as a result of oscillation of the  $C_8H_{11}$  ligand, almost certainly *via* intermediate **5**. The barrier can be estimated to be *ca.*  $12.2 \pm 0.3$  kcal mol<sup>-1</sup>, substantially higher than the value of  $9.1 \pm 0.1$  kcal

<sup>†</sup> Supplementary data available: mass spectral data. For direct electronic access see <http://www.rsc.org/suppdata/dt/1999/3995/>, otherwise available from BLDSC (No. SUP 57649, 3 pp.) or the RSC Library. See Instructions for Authors, 1999, Issue 1 (<http://www.rsc.org/dalton>).

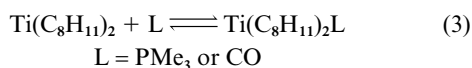


mol<sup>-1</sup> for Fe(2,4-C<sub>7</sub>H<sub>11</sub>)<sub>2</sub>.<sup>7,‡</sup> Possibly the higher value in this case results from the greater apparent substituent tilts in the M(C<sub>8</sub>H<sub>11</sub>)<sub>2</sub> complexes (see below). For **1**, as with Ti(2,4-C<sub>7</sub>H<sub>11</sub>)<sub>2</sub>, much higher barriers were evident, 14.9 ± 0.5 and 15.3 ± 0.2 kcal mol<sup>-1</sup>, respectively.<sup>13§</sup> In these cases, however, theoretical data do not clearly favor either a *syn*- or *anti*-eclipsed intermediate, such as **5** or **6**.<sup>14</sup>



For the fifteen electron V(C<sub>8</sub>H<sub>11</sub>)<sub>2</sub> complex, magnetic susceptibility measurements reveal the presence of the expected one unpaired electron, analogous to that of V(2,4-C<sub>7</sub>H<sub>11</sub>)<sub>2</sub>, but in contrast to the high spin vanadocene.<sup>15</sup> The ESR spectra revealed a characteristic eight line pattern ( $I_v = 7/2$ ), with a vanadium hyperfine splitting of 76.6 G, similar to that of 77.2 G for V(2,4-C<sub>7</sub>H<sub>11</sub>)<sub>2</sub>, while that for V(dmch)<sub>2</sub> is significantly smaller, at 54 G. Overall, these electronically open dienyl complexes display more similarity to each other than to vanadocenes.

As had been observed for various open titanocenes,<sup>16</sup> the fourteen electron Ti(C<sub>8</sub>H<sub>11</sub>)<sub>2</sub> was observed to form 16 electron mono(ligand) adducts with appropriate Lewis bases, eqn. (3).



For example, formation and precipitation of a deep red PMe<sub>3</sub> adduct could be observed at low temperatures (*ca.* -80 °C), although even well below room temperature (*ca.* -30 °C) decoordination occurred. This relatively weak binding contrasts significantly with that for Ti(2,4-C<sub>7</sub>H<sub>11</sub>)<sub>2</sub>(PMe<sub>3</sub>),<sup>17</sup> for which the binding was relatively complete even above room temperature. It is clear that the presence of the two C<sub>3</sub>H<sub>6</sub> bridges in the complexes has greatly impeded the tendency of these molecules to be coordinated by additional ligands, thereby favoring their electron deficient M(C<sub>8</sub>H<sub>11</sub>)<sub>2</sub> forms. Quite analogous observations were also made for the Ti(6,6-dmch)<sub>2</sub> and V(6,6-dmch)<sub>2</sub> complexes.<sup>4</sup> However, stronger binding was achieved with CO, as exposure of Ti(C<sub>8</sub>H<sub>11</sub>)<sub>2</sub> in solution to CO at room temperature led to a change to a paler, apple-green color. The resulting 16 electron mono(carbonyl) adduct **7** could be straightforwardly isolated and characterized. As in the case of Ti(2,4-C<sub>7</sub>H<sub>11</sub>)<sub>2</sub>(CO), but very much unlike Ti(2,4-C<sub>7</sub>H<sub>11</sub>)<sub>2</sub> or Ti(C<sub>8</sub>H<sub>11</sub>)<sub>2</sub>, this complex was found to be air stable for short periods (minutes to hours). The complex also appears stable at room temperature, as opposed to Ti(2,4-C<sub>7</sub>H<sub>11</sub>)<sub>2</sub>(CO). NMR

‡ For **4**, the approximate barrier was obtained from peaks at δ 53.13 and 61.55 in the <sup>13</sup>C NMR spectrum (Δν = 632 Hz), with T<sub>c</sub> = 278 K.

§ For **1**, the approximate barrier was obtained from peaks at δ 87.1160 and 87.1786 in the <sup>13</sup>C NMR spectrum (Δν = 4.7 Hz), with T<sub>c</sub> = 273 K. One can note that the barrier of 10.8 kcal mol<sup>-1</sup> for Ti(6,6-dmch)<sub>2</sub><sup>4</sup> is dramatically lower than those for the other titanium complexes, perhaps a result of a short C1...C5 separation.

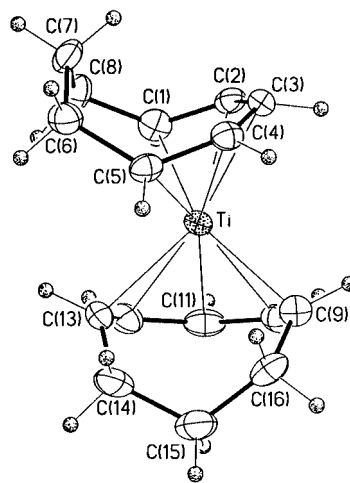
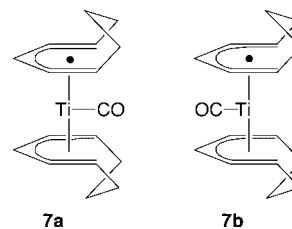
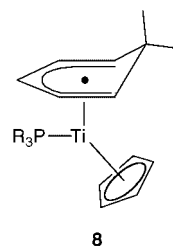


Fig. 1 Perspective view of Ti(C<sub>8</sub>H<sub>11</sub>)<sub>2</sub>.



Spectroscopy for **7** indicated the adoption of a very symmetric pattern, such as **7a** or **7b**. Although structure **7a** would be analogous to all other Ti(2,4-C<sub>7</sub>H<sub>11</sub>)<sub>2</sub>L complexes, as well as to Ti(dmch)<sub>2</sub>(CO), it has been observed that for the edge-bridged half-open titanocenes the incorporation of the additional ligand occurs by the C(3) position, as in **8**, instead of by the



electronically open edge.<sup>18</sup> A structural determination has, however, revealed the actual structure of **7** to be that of **7a** (see below).

Additional interesting insight could be obtained through infrared spectroscopy. The C–O stretching frequency for complex **7** was found to occur at 1879 cm<sup>-1</sup>, compared to values of 1904 cm<sup>-1</sup> for Ti(6,6-dmch)<sub>2</sub>(CO) and 1952 cm<sup>-1</sup> for Ti(2,4-C<sub>7</sub>H<sub>11</sub>)<sub>2</sub>(CO). In this regard, then, the two edge-bridged complexes appear relatively similar, although in color one again observes the red dmch complex to be unique, as the other carbonyl complexes are green. The lower value of the C–O stretching frequency for **7** compared to the dmch complex could be a result of the fact that **7** has effectively a separate alkyl substituent on each of its terminal dienyl positions, whereas in the dmch ligand the two dienyl termini on a given ligand share the same alkyl substituent. Methylation of dienyl termini has in fact been shown to lead to significant reductions in C–O stretching frequencies.<sup>19</sup>

### Structural

Solid state structural studies have confirmed the formulations of complexes **1–4**. Pertinent bonding parameters are provided in Tables 1–4, and perspective views are presented in Figs. 1–4.

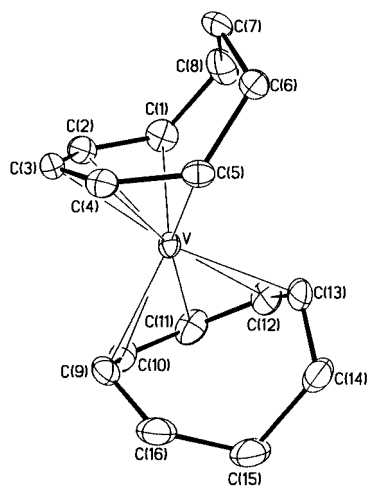


Fig. 2 Perspective view of  $V(C_8H_{11})_2$ .

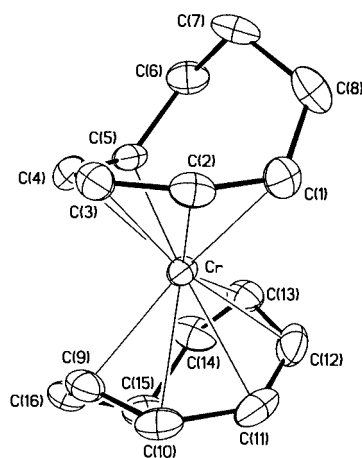


Fig. 3 Perspective view of  $Cr(C_8H_{11})_2$ .

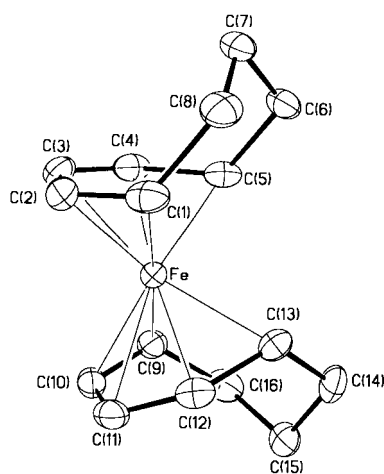


Fig. 4 Perspective view of  $Fe(C_8H_{11})_2$ .

A comparative summary of selected geometrical parameters is given in Table 5. As can be seen, the approximate conformations of the Ti (**1**) and Fe (**4**) complexes correspond to the  $90^\circ$  staggered and  $60^\circ$  gauche-eclipsed forms, depicted above. Other edge-bridged iron<sup>20</sup> and ruthenium<sup>21</sup> complexes adopt structures similar to that of **4**. The vanadium complex **2** also adopts the staggered conformation, while that of **3** is intermediate between **1** and **4**. The observed conformations are quite similar to those adopted by the  $M(2,4-C_7H_{11})_2$  species ( $M = V, 89.8$ ;  $Cr, 82.2$ ;  $Fe, 59.7^\circ$ ).<sup>1</sup> A similar correspondence is observed for the "fold" angles, defined by the angle between the  $M-C(1)-C(5)$  and  $C(1)-C(5)$  planes. In each case the value for a given

Table 1 Selected bond distances ( $\text{\AA}$ ) and angles ( $^\circ$ ) for  $Ti(C_8H_{11})_2$

Ti–C(1)	2.220(6)	Ti–C(9)	2.218(7)
Ti–C(2)	2.262(6)	Ti–C(10)	2.262(6)
Ti–C(3)	2.284(6)	Ti–C(11)	2.264(7)
Ti–C(4)	2.237(6)	Ti–C(12)	2.242(6)
Ti–C(5)	2.226(6)	Ti–C(13)	2.236(6)
C(1)–C(2)	1.419(8)	C(9)–C(10)	1.398(9)
C(2)–C(3)	1.404(9)	C(10)–C(11)	1.413(9)
C(3)–C(4)	1.425(8)	C(11)–C(12)	1.425(10)
C(4)–C(5)	1.402(8)	C(12)–C(13)	1.387(11)
C(1)–C(2)–C(3)	128.5(6)	C(9)–C(10)–C(11)	128.6(7)
C(2)–C(3)–C(4)	130.1(5)	C(10)–C(11)–C(12)	130.7(7)
C(3)–C(4)–C(5)	128.6(5)	C(11)–C(12)–C(13)	128.0(6)

Table 2 Selected bond distances ( $\text{\AA}$ ) and angles ( $^\circ$ ) for  $V(C_8H_{11})_2$

V–C(1)	2.169(3)	V–C(9)	2.175(3)
V–C(2)	2.206(3)	V–C(10)	2.214(3)
V–C(3)	2.242(3)	V–C(11)	2.238(4)
V–C(4)	2.187(3)	V–C(12)	2.192(3)
V–C(5)	2.182(3)	V–C(13)	2.185(3)
C(1)–C(2)	1.403(4)	C(9)–C(10)	1.405(5)
C(2)–C(3)	1.416(5)	C(10)–C(11)	1.399(5)
C(3)–C(4)	1.408(5)	C(11)–C(12)	1.418(5)
C(4)–C(5)	1.409(4)	C(12)–C(13)	1.397(6)
C(1)–C(2)–C(3)	127.8(4)	C(9)–C(10)–C(11)	129.0(4)
C(2)–C(3)–C(4)	130.2(3)	C(10)–C(11)–C(12)	129.9(4)
C(3)–C(4)–C(5)	128.7(3)	C(11)–C(12)–C(13)	129.2(4)

Table 3 Selected bond distances ( $\text{\AA}$ ) and angles ( $^\circ$ ) for  $Cr(C_8H_{11})_2$

Cr–C(1)	2.207(7)	Cr–C(9)	2.188(7)
Cr–C(2)	2.172(7)	Cr–C(10)	2.182(8)
Cr–C(3)	2.187(7)	Cr–C(11)	2.191(8)
Cr–C(4)	2.135(7)	Cr–C(12)	2.137(7)
Cr–C(5)	2.160(6)	Cr–C(13)	2.152(7)
C(1)–C(2)	1.429(10)	C(9)–C(10)	1.406(11)
C(2)–C(3)	1.395(11)	C(10)–C(11)	1.421(13)
C(3)–C(4)	1.410(10)	C(11)–C(12)	1.417(12)
C(4)–C(5)	1.414(10)	C(12)–C(13)	1.397(13)
C(1)–C(2)–C(3)	127.8(8)	C(9)–C(10)–C(11)	126.4(8)
C(2)–C(3)–C(4)	129.1(6)	C(10)–C(11)–C(12)	128.1(8)
C(3)–C(4)–C(5)	126.6(7)	C(11)–C(12)–C(13)	127.8(7)

Table 4 Selected bond distances ( $\text{\AA}$ ) and angles ( $^\circ$ ) for  $Fe(C_8H_{11})_2$

Fe–C(1)	2.126(7)	Fe–C(9)	2.111(6)
Fe–C(2)	2.055(6)	Fe–C(10)	2.068(6)
Fe–C(3)	2.110(6)	Fe–C(11)	2.112(6)
Fe–C(4)	2.067(6)	Fe–C(12)	2.056(5)
Fe–C(5)	2.072(5)	Fe–C(13)	2.079(5)
Fe'–C(1')	2.120(6)	Fe'–C(9')	2.134(6)
Fe'–C(2')	2.070(5)	Fe'–C(10')	2.065(7)
Fe'–C(3')	2.116(5)	Fe'–C(11')	2.119(7)
Fe'–C(4')	2.060(5)	Fe'–C(12')	2.062(6)
Fe'–C(5')	2.077(6)	Fe'–C(13')	2.090(6)
C(1)–C(2)	1.385(9)	C(9)–C(10)	1.406(8)
C(2)–C(3)	1.401(10)	C(10)–C(11)	1.424(9)
C(3)–C(4)	1.408(9)	C(11)–C(12)	1.382(9)
C(4)–C(5)	1.420(8)	C(12)–C(13)	1.423(7)
C(1')–C(2')	1.421(8)	C(9')–C(10')	1.417(8)
C(2')–C(3')	1.412(7)	C(10')–C(11')	1.420(8)
C(3')–C(4')	1.402(7)	C(11')–C(12')	1.410(9)
C(4')–C(5')	1.434(7)	C(12')–C(13')	1.429(9)
C(1)–C(2)–C(3)	125.2(6)	C(9)–C(10)–C(11)	124.0(6)
C(2)–C(3)–C(4)	125.9(6)	C(10)–C(11)–C(12)	125.5(5)
C(3)–C(4)–C(5)	126.4(6)	C(11)–C(12)–C(13)	128.2(6)
C(1')–C(2')–C(3')	122.9(5)	C(9')–C(10')–C(11')	124.6(6)
C(2')–C(3')–C(4')	125.6(5)	C(10')–C(11')–C(12')	124.5(6)
C(3')–C(4')–C(5')	127.6(5)	C(11')–C(12')–C(13')	128.4(5)

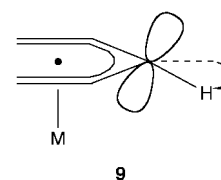
**Table 5** Comparisons of averaged structural parameters (distances in Å, angles in °) for the  $M(C_8H_{11})_2$ 

Parameter	Ti	V	Cr	Fe
Conformation angle	88.4	89.7	84.0	58.4
Interligand tilt	28.5	21.2	24.5	22.7
C(1)···C(5)	3.238	3.231	3.115	2.947
M–CM	1.643	1.584	1.563	1.480
M–C(1), C(5)	2.225(4)	2.178(3)	2.177(10) <sup>a</sup>	2.101(11) <sup>a</sup>
M–C(2), C(4)	2.251(3)	2.200(4)	2.156(10) <sup>a</sup>	2.062(2)
M–C(3)	2.274(4)	2.240(2)	2.189(5)	2.114(3)
M–C (average)	2.245	2.199	2.171	2.088
C(1)–C(2)–C(3)	128.4(3)	128.7(2)	127.2(4)	126.0(9) <sup>a</sup>
C(2)–C(3)–C(4)	130.4(4)	130.1(2)	128.6(5)	125.4(3)
C(1)–C(8)–C(7)	117.0(3)	116.4(2)	116.5(4)	116.0(2)
C(6)–C(7)–C(8)	114.4(5)	113.5(2)	113.0(4)	110.0(3)
C(2)–C(1)–C(8)	126.1(4)	127.0(2)	127.5(4)	126.7(3)
C–C (deloc., average)	1.410	1.407	1.411	1.412
C(6), C(8) tilts <sup>b</sup>	59.4 (46.3)	57.8 (46.0)	61.3 (47.9)	66.9 (52.0)
Hydrogen tilts	25.3	26.8	24.8	24.6
Fold angle	80.1	79.8	75.0	70.6

<sup>a</sup> In this case, individual values being averaged differ from one side of the ligand to the other. <sup>b</sup> The first tilt value in each case is derived from the appropriate torsion angle; the sine of the second value is equal to the deviation of a given atom, C(6) or C(8), from the dienyl least-squares plane divided by the C(1)–C(6) or C(5)–C(8) distance.

$M(C_8H_{11})_2$  complex is within 3° of that for the corresponding  $M(2,4-C_7H_{11})$  complex (V, 78.8; Cr, 72.9; Fe, 68.1°).<sup>22</sup> Much of the similarity between **1–4** and the 2,4- $C_7H_{11}$  analogs may arise from a notable flexibility of the  $C_8H_{11}$  ligand. As can be seen in Table 5, the C(1)···C(5) separation is quite variable, ranging from 3.238 to 2.947 Å for **1–4**. This is surprising both in its variability and in its similarity to those of the  $M(2,4-C_7H_{11})_2$  complexes (V, 3.05; Cr, 2.93; Fe, 2.785 Å). Thus, in both cases the girth of the dienyl ligand contracts for smaller metal centers in order to maintain effective overlap. It can be observed that the bridge does lead to a fairly regular expansion of the open edge separation by 0.16–0.18 Å, but this seems to be of a small enough magnitude that the complexes' electronic and conformational properties are relatively unchanged. While structural data for the  $M(6,6-dmch)_2$  complexes do not seem available, it is worth noting that the C(1)···C(5) separation for the 6,6-dmch ligand is significantly less than those for either of the other electronically open ligands (*cf.*,  $Ti(C_5H_5)(6,6-dmch)(PMe_3)$ , 2.34;  $Ti(C_5H_4CH_3)(C_8H_{11})(PEt_3)$ , 3.075;  $Ti(C_5H_5)(2,4-C_7H_{11})(PEt_3)$ , 3.09 Å). This most likely accounts for the differences in colors and ESR spectral parameters displayed by the 6,6-dmch complexes (see above).

The expansion of the open edge length does lead to some other geometrical effects, including an increase in the average delocalized C–C–C bond angles (*ca.* 2°), and a decrease of *ca.* 0.03–0.05 Å in the M–CM (center of mass) distance. However, there is one structural aspect in which one sees a fairly significant change relative to the  $M(2,4-C_7H_{11})_2$  complexes, namely the degree of bending experienced by the various substituents. The methylene groups adjacent to the dienyl fragment experience deviations of some 58–67° out of the dienyl plane, away from the metal centers. This, as well as the greater girth of these ligands, may then lead to enhanced deviations (toward the metal center) by the hydrogen atom substituents on the delocalized (C(1)–C(5)) carbon atoms, relative to the  $M(2,4-C_7H_{11})_2$  complexes. Deviations of these types, but of generally smaller magnitudes, are expected, and have been attributed to attempts by the ligand to improve overlap with the transition metal system.<sup>23</sup> For the dienyl group's terminal carbon atoms, one can relate the distortions to an approach to  $sp^3$  hybridization for these atoms,<sup>24</sup> as well as to an attempt to relieve intramolecular H···H interactions,<sup>25</sup> while for the dienyl group's internal carbon atoms the substituent tilts have been attributed to an attempt to tilt the atom's p orbital more toward the metal center, as in **9**. It is possible that the initial, large downward tilt by the hydrogen atom substituents on the terminal carbon atoms (C(1), C(5)) may then enhance the tilts of the other hydro-



gen atom substituents in order to optimize overlap between adjacent, formal p orbitals in the delocalized  $\pi$  system. One final point of interest concerning the  $C_3H_6$  bridge is its consistent folding back over the dienyl ligand. Most likely this orientation is favored due to the resulting C–H/ $\pi$  interaction.<sup>26</sup> The exposure of one C–H bond to the dienyl fragment's  $\pi$  electron density can clearly be seen through a significant upfield shift for one resonance in the <sup>1</sup>H NMR spectrum.

The average M–C bond distances also parallel those of the  $M(2,4-C_7H_{11})_2$  compounds (V, 2.211; Cr, 2.163; Fe, 2.089 Å). Of course, since these are each averages of several different types of bonds, exact comparisons cannot be drawn. However, the fact that the averages for the  $M(2,4-C_7H_{11})_2$  and  $M(C_8H_{11})_2$  complexes are within *ca.* 0.01 Å of each other provides an indication that comparisons would likely be valid nonetheless. To begin with, one can observe a steady increase in M–C bond distance as one moves further from the 18 electron configuration of  $Fe(C_8H_{11})_2$ . A similar trend exists for the metallocenes (see Contents graphic), which has been characterized as an “electron imbalance” relationship.<sup>23b</sup> However, while the appropriate, average M–C distances in  $M(2,4-C_7H_{11})_2$  and  $M(C_8H_{11})_2$  complexes are similar to those of chromocene and ferrocene, those for the low spin complexes **1** and **2** are much shorter than in metallocenes of vanadium (2.199 *vs.* 2.280 Å) and titanium (2.245 *vs.* 2.352 Å).<sup>12,27</sup> Although it is clear that spin configurations can have a large effect on bond distances, such that comparably stable species may have much differing bond distances (*e.g.*, manganocenes<sup>28</sup>), structural data for half-open metallocenes of titanium,<sup>2a</sup> vanadium,<sup>29</sup> even chromium<sup>30</sup> and more recently zirconium<sup>31</sup> have demonstrated that such differences persist even when the two ligands are present in the same complex, and hence are no longer subject to spin state differences. Theoretical calculations have substantiated expectations of stronger bonding for the pentadienyl ligand, and have revealed that the open ligands engender a much greater degree of metal–ligand orbital mixing, and furthermore generally serve as much stronger electron acceptors, through a significant  $\delta$  interaction.

Although the presence of the edge bridge may alter inherent bonding patterns of the ligand, some useful information may

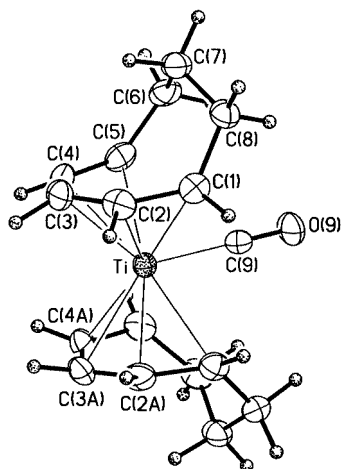


Fig. 5 Perspective view of  $\text{Ti}(\text{C}_8\text{H}_{11})_2(\text{CO})$ .

still be derived from trends displayed within the  $\text{M}(\text{C}_8\text{H}_{11})_2$  series. Unlike the  $\text{M}(2,4\text{-C}_7\text{H}_{11})_2$  series, however, the central carbon atoms (C(3), C(11)) are consistently most remotely positioned from their metal centers. As a result, the most important trends to observe involve the C(1), C(5) and C(2), C(4) positions. As had been observed for the  $\text{M}(2,4\text{-C}_7\text{H}_{11})_2$  series (V, Cr, Fe), for the early metals, V and presumably Ti, the shortest M–C interactions involve the formally charged C(1), C(5) positions, whereas for Fe the preference shifts to the formally uncharged C(2), C(4) positions. In both series the chromium complex has relatively comparable M–C distances for all positions. This general trend can be accounted for through arguments based on the relative favorabilities of  $\text{M} \rightarrow \text{L}$  and  $\text{L} \rightarrow \text{M}$  bonding interactions. For the earlier metals one can propose that the most important interaction would be  $\pi$  ( $\text{L} \rightarrow \text{M}$ ), which would be expected heavily to utilize the formally charged carbon atoms, e.g., C(1), C(5). In contrast, for the later metals, especially iron, additional metal electrons would be available in orbitals which could lead to strong  $\delta$  M–L backbonding interactions. The ligand atoms most prone to adopting an acceptor role would naturally be the uncharged C(2), C(4) positions, thus leading to short Fe–C(2), C(4) distances. These arguments are also nicely consistent with the observed structures of the molecules, as the  $90^\circ$  conformation of the early complexes leads to a correspondence of the angle between the two ligands'  $\pi$  MOs and the angle between the potential  $\pi$  accepting  $d_{xz}$  and  $d_{yz}$  orbitals of the metal center. For the later iron complex an eclipsed conformation could be considered to be a result of the  $\delta$  bonding interactions, although it can also be noted that in a *gauche*-eclipsed conformation an octahedral arrangement of the formally charged C(1), C(3), C(5) positions results. However, this would also be the case for an *anti*-eclipsed conformation, **6**, which appeared to be the more stable form from molecular orbital studies.<sup>2b</sup> It is still not clear what leads to the stabilization of the *gauche*-eclipsed form relative to *anti*-eclipsed for the iron complexes, although several subtle factors could play a role.¶

The structure of  $\text{Ti}(\text{C}_8\text{H}_{11})_2(\text{CO})$  **7** was determined in order to establish the location of CO attachment (Fig. 5, Table 6). As noted earlier, in  $\text{Ti}(2,4\text{-C}_7\text{H}_{11})_2\text{L}$  complexes, the additional ligands had invariably been located by the electronically open edge, whereas in  $\text{Ti}(\text{C}_5\text{H}_5)(\text{C}_8\text{H}_{11})(\text{PEt}_3)$  (and its 6,6-dmch analog) the presence of the edge bridge appears to have forced the additional ligands to be positioned by the C(3) location,<sup>18</sup> as in **7a**. The observed structure for  $\text{Ti}(\text{C}_8\text{H}_{11})_2(\text{CO})$  clearly reveals that CO has occupied a position between the electronically

¶ Some possibilities include a favorable HOMO/LUMO arrangement between the two dienyl fragments, a greater extent of orbital mixing that is allowed by the lower symmetry arrangement, and the ability for the two ligands to tilt away from a parallel orientation.

Table 6 Selected bond distances (Å) and angles ( $^\circ$ ) for  $\text{Ti}(\text{C}_8\text{H}_{11})_2(\text{CO})$

Ti–C(1)	2.362(3)	Ti–C(4)	2.261(3)
Ti–C(2)	2.270(4)	Ti–C(5)	2.365(4)
Ti–C(3)	2.286(4)	Ti–C(9)	1.979(5)
C(1)–C(2)	1.404(4)	C(4)–C(5)	1.415(5)
C(1)–C(8)	1.499(5)	C(5)–C(6)	1.500(5)
C(2)–C(3)	1.407(5)	C(6)–C(7)	1.512(5)
C(3)–C(4)	1.403(5)	C(7)–C(8)	1.495(5)
C(9)–O(9)	1.142(5)		
C(8)–C(1)–C(2)	125.5(3)	C(4)–C(5)–C(6)	126.7(3)
C(1)–C(2)–C(3)	128.1(3)	C(5)–C(6)–C(7)	116.2(3)
C(2)–C(3)–C(4)	128.5(3)	C(6)–C(7)–C(8)	114.0(3)
C(3)–C(4)–C(5)	128.7(3)	C(7)–C(8)–C(1)	117.4(3)

open edges. Apparently, it would be worse to have the two edge bridges forced to lie directly beside each other, as in **7b**. At first glance, there would not seem to be significant steric interactions between the edge bridges and the carbonyl ligands as there is only a  $2^\circ$  angle between the two dienyl ligand planes. However, the dienyl ligands actually are significantly non-planar, and adopt something close to an envelope conformation, with an angle of  $8.3^\circ$  formed between the C(2)–C(3)–C(4) and the C(1)–C(2)–C(4)–C(5) planes. This leads to a greater separation between the terminal carbon atoms of one dienyl fragment and those of the other, and also is likely responsible for the fact that the average Ti–C(1), C(5) distance is significantly longer than those for the C(2), C(4) and C(3) positions, 2.364(2) vs. 2.272(2) and 2.286(4) Å, respectively. Overall, these distances are lengthened relative to those in the 14 electron parent **1**. The Ti–CM distance is also correspondingly lengthened, being 1.746 Å. The Ti–CO distance of 1.979(5) Å is comparable to that of 1.978(9) Å for  $\text{Ti}(6,6\text{-dmch})_2(\text{CO})$ .

The edge-bridged 6,6-dimethylcyclohexadienyl and cyclooctadienyl ligands add an extra dimension to metal–dienyl chemistry,<sup>32</sup> being intermediate in their physical properties between pentadienyl and cyclopentadienyl ligands. The edge-bridged complexes are also significantly more sterically demanding, which should make them ideal for stabilizing electron deficient species. An additional advantage of these ligands appears to be their greater ease of crystallization. However, it is also clear that there are significant differences between various edge-bridged ligands, most likely traceable to the differing separations between their terminal (C(1), C(5)) carbon atoms. It would seem that much remains to be gained from additional studies involving a broader range of edge-bridged ligands.

## Experimental

All reactions were carried out under a nitrogen atmosphere in Schlenk apparatus. Ether and hydrocarbon solvents were distilled from sodium–benzophenone under a nitrogen atmosphere. The compound  $\text{K}(\text{C}_8\text{H}_{11})$  was prepared according to a general method for pentadienyl anions.<sup>33</sup> Spectroscopic data were obtained as previously described.<sup>34</sup> The  $^1\text{H}$  and  $^{13}\text{C}$  NMR spectra were obtained at 300 and 75 MHz, respectively. For the  $^{13}\text{C}$  NMR spectra the peaks were not precisely integrated, but numbers of carbon atoms are presented in accord with their assignments. Elemental analyses were obtained from Robertson Microlit. Mass spectral data are available as supplementary material.

## Preparation

**Bis(cyclooctadienyl)titanium,  $\text{Ti}(\eta^5\text{-C}_8\text{H}_{11})_2$ .** To a frozen mixture of 50 mL THF and 70–80 mesh magnesium metal (0.88 g, 36 mmol) was added  $\text{TiCl}_4$  (3.3 mL, 30 mmol). The mixture was allowed to warm to room temperature and then refluxed for 1.5 h to give a black slurry of “ $\text{TiCl}_2$ ”. The slurry was then cooled to  $-78^\circ\text{C}$  and a solution of  $\text{K}(\text{C}_8\text{H}_{11})$  (8.8 g, 60 mmol) in 50

**Table 7** X-Ray data parameters for  $\text{Ti}(\text{C}_8\text{H}_{11})_2$ ,  $\text{V}(\text{C}_8\text{H}_{11})_2$ ,  $\text{Cr}(\text{C}_8\text{H}_{11})_2$ ,  $\text{Fe}(\text{C}_8\text{H}_{11})_2$ , and  $\text{Ti}(\text{CH}_{11})_2(\text{CO})$ 

Formula	$\text{C}_{16}\text{H}_{22}\text{Ti}$	$\text{C}_{16}\text{H}_{22}\text{V}$	$\text{C}_{16}\text{H}_{22}\text{Cr}$	$\text{C}_{16}\text{H}_{22}\text{Fe}$	$\text{C}_{17}\text{H}_{22}\text{OTi}$
<i>M</i>	262.24	265.28	266.34	270.19	290.25
Crystal system	Orthorhombic	Orthorhombic	Orthorhombic	Triclinic	Monoclinic
Space group	$P2_12_12_1$	$P2_12_12_1$	$P2_12_12_1$	$P\bar{1}$	$P2_1/m$
<i>T</i> /K	298	218	298	249	298
<i>a</i> /Å	9.608(4)	9.4927(9)	9.614(2)	7.306(3)	6.998(2)
<i>b</i> /Å	9.893(2)	9.8940(9)	9.850(1)	13.327(4)	16.263(2)
<i>c</i> /Å	13.981(2)	14.0614(12)	13.923(3)	13.861(3)	7.055(1)
$\alpha^\circ$				98.25(2)	
$\beta^\circ$				97.51(2)	115.88(1)
$\gamma^\circ$				100.57(2)	
<i>V</i> /Å <sup>3</sup>	1328.9(6)	1320.7(3)	1318.5(4)	1295.8(7)	722.4(3)
<i>Z</i>	4	4	4	4	2
$\mu/\text{cm}^{-1}$	6.19	7.26	8.43	11.38	5.82
Data collected	1832	4371	1824	4288	1358
Unique data with $I > n\sigma(I)$ ; <i>n</i>	1681; 2	2848; 2	1677; 2	3323; 2	982; 2
<i>R</i> ( <i>F</i> )	0.049	0.039	0.047	0.054	0.043
<i>R</i> <sub>w</sub> ( <i>F</i> )	0.072	0.076	0.142	0.112	0.104

mL THF added dropwise. The mixture was warmed to room temperature and stirred overnight during which time a very dark green solution resulted. Next, the solvent was removed *in vacuo* and the black-green residue extracted into three 100 mL portions of pentane and filtered through a Celite pad on a coarse frit. Concentration of the green filtrate *in vacuo* to ca. 100 mL and placement into a  $-20^\circ\text{C}$  freezer gave 2.2 g (28%) of the complex as air-sensitive dark green needle-shaped crystals. Melting point (nitrogen-filled sealed capillary): 110–112 °C. Calc. for  $\text{C}_{16}\text{H}_{22}\text{Ti}$ : C, 73.28; H, 8.45. Found: C, 72.96; H, 8.37%. <sup>1</sup>H NMR (toluene-*d*<sub>8</sub>, ambient):  $\delta$  7.17 (t, 1 H, *J* = 10.7, H-3), 6.74 (t, 1 H, *J* = 10.9, H-2), 4.74 (t, 1 H, *J* = 11.7, H-4), 4.05 (dd, 1 H, *J* = 6.7, 6.3, H-1), 2.77 (m, 1 H, H-6), 1.73 (dd, 1 H, *J* = 7.4, 7.3, H-5), 1.42 (m, 1 H, H-8), 1.26 (tt, 1 H, *J* = 13.6, 2.1, H-6'), 0.71 (m, 1 H, H-8'), 0.43 (qt, 1 H, *J* = 13.6, 2.1, H-7') and  $-0.62$  (t, 1 H, *J* = 13.4 Hz, H-7). <sup>13</sup>C NMR (toluene-*d*<sub>8</sub>, ambient):  $\delta$  128.2 (dt, 2C, *J* = 161, 11, C-3), 106.4 (dt, 4C, *J* = 61, 9, C-2 or 4), 105.7 (dt, 2C, *J* = 160, 9, C-2 or 4), 87.3 (d, 4C, *J* = 148, C-1,5), 38.4 (t, 2C, C-6 or 8), 30.8 (t, 2C, *J* = 127, C-6 or 8) and 20.5 (t, 2C, *J* = 126 Hz, C-7).

**Bis(cyclooctadienyl)titanium monocarbonyl,  $\text{Ti}(\eta^5\text{-C}_8\text{H}_{11})_2(\text{CO})$ .** Over an emerald green solution of  $\text{Ti}(\eta^5\text{-C}_8\text{H}_{11})_2$  (0.50 g, 20 mmol) in 20 mL pentane under a blanket of nitrogen was passed a stream of CO at  $-78^\circ\text{C}$ . After 10 min a distinct change to light green occurred. The reaction mixture was warmed to room temperature and the solvent removed *in vacuo* to give a green solid. This green residue was extracted into two 50 mL portions of pentane and filtered through a Celite pad on a coarse frit. Concentration *in vacuo* of the green filtrate to ca. 20 mL and placement into a  $-20^\circ\text{C}$  freezer gave 0.50 g (91%) of the complex as air-sensitive light green diamond-shaped crystals. Melting point (nitrogen-filled sealed capillary): 133–135 °C. Calc. for  $\text{C}_{17}\text{H}_{22}\text{OTi}$ : C, 70.34; H, 7.64. Found: C, 70.13; H, 7.67%. <sup>1</sup>H NMR (toluene-*d*<sub>8</sub>, ambient):  $\delta$  5.58 (t, 2 H, *J* = 9.4, H-3), 3.94 (dd, 4 H, *J* = 10.8, 10.3, H-2,4), 2.91 (dd, 4 H, *J* = 5.8, 5.6, H-1,5), 2.31 (m, 4 H, H-6,8), 2.24 (qt, 4 H, *J* = 13.2, 2.3, H-6',8'), 0.97 (d, 2 H, *J* = 13.6, H-7) and 0.03 (qt, 2 H, *J* = 13.3, 3.1 Hz, H-7'). <sup>13</sup>C NMR (toluene-*d*<sub>8</sub>, ambient):  $\delta$  253.0 (s, 1C, CO), 116.3 (dt, 2C, *J* = 161, 11, C-3), 102.1 (dt, 4C, *J* = 158, 9, C-2,4), 72.8 (d, 4C, *J* = 148, C-1,5), 30.8 (t, 4C, *J* = 126, C-6,8) and 20.2 (t, 2C, *J* = 126 Hz, C-7). IR (Nujol mull): 1879  $\text{cm}^{-1}$  (CO).

**Bis(cyclooctadienyl)vanadium,  $\text{V}(\eta^5\text{-C}_8\text{H}_{11})_2$ .** A solution of  $\text{VCl}_3 \cdot 3\text{THF}$  (1.0 g, 2.7 mmol) in 30 mL of THF was cooled to  $-78^\circ\text{C}$ . A solution of  $\text{K}(\text{C}_8\text{H}_{11})$  (1.27 g, 8.3 mmol) in 30 mL of THF was slowly added. The resulting black solution was slowly warmed to room temperature. After stirring overnight, the solvent was removed *in vacuo*. The crude product was extracted with three 25 mL portions of pentane, and filtered through a

Celite pad on a coarse frit. The solution was cooled to  $-30^\circ\text{C}$ , yielding a dark green air-sensitive crystalline solid (60% yield). Single crystals were obtained by slowly cooling their concentrated solutions in pentane. Melting point (nitrogen-filled sealed capillary): 95 °C (decomp.). Calc. for  $\text{C}_{16}\text{H}_{22}\text{V}$ : C, 72.44; H, 8.36. Found: C, 71.60; H, 8.39%. Magnetic susceptibility (Evans method,<sup>35</sup> THF):  $1.6 \mu_{\text{B}}$ . ESR (hexane,  $20^\circ\text{C}$ ):  $g = 1.976$ ;  $A_{\text{V}} = 75.7 \text{ G}$ .

**Bis(cyclooctadienyl)chromium,  $\text{Cr}(\eta^5\text{-C}_8\text{H}_{11})_2$ .** A solution of  $\text{CrCl}_2$  (0.80 g, 6.5 mmol) in 30 mL of THF was cooled to  $-78^\circ\text{C}$ . A solution of  $\text{K}(\text{C}_8\text{H}_{11})$  (2.0 g, 14 mmol) in 30 mL of THF was slowly added. The resulting orange-brown solution was slowly warmed to room temperature. After stirring overnight, the solvent was removed *in vacuo* from the black solution. The crude product was extracted with three 25 mL portions of pentane, and then filtered through a Celite pad on a coarse frit. The solution was cooled to  $-30^\circ\text{C}$ , yielding a dark green air-sensitive crystalline solid (70–80% yield). Single crystals were obtained by slowly cooling their concentrated solutions in pentane.

**Bis(cyclooctadienyl)iron,  $\text{Fe}(\eta^5\text{-C}_8\text{H}_{11})_2$ .** To a magnetically stirred slurry of  $\text{FeCl}_3$  (1.00 g, 6.17 mmol) in 20 mL of THF at  $-78^\circ\text{C}$  was slowly added a solution of  $\text{K}(\text{C}_8\text{H}_{11})$  (2.83 g, 19.1 mmol) in 40 mL of THF. After addition was complete the solution was allowed to warm to room temperature and stirred overnight. Then, the solvent was removed *in vacuo* from the dark brown solution. The residue was extracted with pentane and filtered through a Celite pad on a coarse frit. The product was isolated by cooling to  $-90^\circ\text{C}$ , as an orange crystalline solid (65–70% yield). Melting point (nitrogen-filled sealed capillary): 81–83 °C. Calc. for  $\text{C}_{16}\text{H}_{22}\text{Fe}$ : C, 71.12; H, 8.21. Found: C, 71.21; H, 8.37%. <sup>1</sup>H NMR (toluene-*d*<sub>8</sub>, ambient,  $-35^\circ\text{C}$ ):  $\delta$  5.11 (t, 1 H, H-3), 3.48 (m, 2 H, H-2, H-4), 2.50 (d, 2 H, H-1, H-5), 2.15 (t, 1 H, H-6, *J* = 12.9), 1.61 (br, 1H, H-6'), 1.38 (m, 1 H, H-8), 1.17 (m, 1 H, H-8'), 0.94 (m, 1 H, H-7) and  $-0.25$  (q, 1 H, H-7', *J* = 12.9 Hz). <sup>13</sup>C NMR (toluene-*d*<sub>8</sub>, ambient,  $-35^\circ\text{C}$ ):  $\delta$  105.5 (d, C-3, *J* = 150), 90.9 (d, C-2, *J* = 157), 79.9 (d, C-4, *J* = 159), 61.6 (d, C-1, *J* = 145), 53.1 (d, C-5, *J* = 145 Hz), 30.2 (t, C-6 and C-8, *J* = 119) and 28.8 (t, C-7, *J* = 118 Hz).

#### Structural studies

Crystals of the compounds studied were grown by slowly cooling concentrated solutions in hydrocarbons. They were subsequently mounted in glass capillaries under nitrogen atmospheres, and transferred to a Siemens P4 or P4/CCD diffractometer, each of which utilized a Mo-*K* $\alpha$  source ( $\lambda = 0.71073 \text{ \AA}$ ). Diffraction symmetries and systematic absences for several of the  $\text{M}(\text{C}_8\text{H}_{11})_2$  complexes ( $\text{M} = \text{Ti}, \text{V}$  or  $\text{Cr}$ ) were uniquely

consistent for the space group  $P2_12_12_1$ , while for  $\text{Fe}(\text{C}_8\text{H}_{11})_2$  and  $\text{Ti}(\text{C}_8\text{H}_{11})_2(\text{CO})$ , the respective space groups  $P\bar{1}$  and  $P2_1/m$  were suggested by intensity statistics and confirmed by their successful refinements. For the isomorphous  $\text{M}(\text{C}_8\text{H}_{11})_2$  ( $\text{M} = \text{Ti}, \text{V}$  or  $\text{Cr}$ ) complexes, refinements of the Flack parameters suggested that enantiomorphic mixtures were present (44/56, 55/45, and 30/70, respectively). For  $\text{Fe}(\text{C}_8\text{H}_{11})_2$ , two independent molecules were present but their structural parameters were nearly identical. Non-hydrogen atoms were refined anisotropically, while hydrogen atoms were treated as idealized contributions. Other data collection and refinement parameters are presented in Table 7.

CCDC reference number 186/1662.

## Acknowledgements

R. D. E. is grateful to the University of Utah and the National Science Foundation for partial support of this work.

## References

- 1 R. D. Ernst, *Chem. Rev.*, 1988, **88**, 1255.
- 2 (a) I. Hyla-Kryspin, T. E. Waldman, E. Meléndez, W. Trakarnpruk, A. M. Arif, M. L. Ziegler, R. D. Ernst and R. Gleiter, *Organometallics*, 1992, **11**, 3201; (b) M. C. Böhm, M. Eckert-Maksić, R. D. Ernst, D. R. Wilson and R. Gleiter, *J. Am. Chem. Soc.*, 1982, **104**, 2699; (c) R. M. Kowaleski, F. Basolo, J. H. Osborne and W. C. Trogler, *Organometallics*, 1988, **7**, 1425.
- 3 J. F. Helling and D. M. Braitsch, *J. Am. Chem. Soc.*, 1970, **92**, 7207, 7209.
- 4 P. T. DiMauro and P. T. Wolczanski, *Organometallics*, 1987, **6**, 1947.
- 5 J. Mueller and B. Mertschenk, *Chem. Ber.*, 1972, **105**, 3346; J. Müller, W. Holzinger and F. H. Köhler, *Chem. Ber.*, 1976, **109**, 1222.
- 6 P. Pertici, G. Vitalli, M. Paci and L. Porri, *J. Chem. Soc., Dalton Trans.*, 1980, 1961.
- 7 D. R. Wilson, R. D. Ernst and T. H. Cymbaluk, *Organometallics*, 1983, **2**, 1220.
- 8 J. T. Spencer and R. D. Ernst, *US Pat.*, 5 352 488, 1994.
- 9 S. J. Severson, T. H. Cymbaluk, R. D. Ernst, J. M. Higashi and R. W. Parry, *Inorg. Chem.*, 1983, **22**, 3833; T. D. Newbound, J. W. Freeman, D. R. Wilson, M. S. Kralik, A. T. Patton, C. F. Campana and R. D. Ernst, *Organometallics*, 1987, **6**, 2432; M. C. Böhm, R. D. Ernst, R. Gleiter and D. R. Wilson, *Inorg. Chem.*, 1983, **22**, 3815.
- 10 B. Hessen, T. Siegrist, T. Palstra, S. M. Tanzler and M. L. Steigerwald, *Inorg. Chem.*, 1993, **32**, 5165; B. Hessen, S. M. Stuczynski and M. L. Steigerwald, Presented at the 205th National ACS Meeting, Denver, Colorado, March 28, 1993.
- 11 J. W. Freeman, D. R. Wilson, R. D. Ernst, P. D. Smith, D. D. Klendworth and M. P. McDaniel, *J. Polym. Sci. A*, 1987, **25**, 2063; P. D. Smith and M. P. McDaniel, *J. Polym. Sci. A*, 1989, **27**, 2695; G. M. Dawkins, *Eur. Pat. Appl.*, 0416785A2, 1991, 0416786A2, 1991 and 0501672, 1993; T. Kohara and S. Ueki, *US Pat.*, 4 871 704, 1989; 4 926 502, 1990; M. B. Zielinski, *US Pat.*, 5 075 426, 1991; P. D. Smith and E. Hsieh, *US Pat.*, 4 587 227, 1986; E. A. Benham, P. D. Smith, E. T. Hsieh and M. P. McDaniel, *J. Macromol. Sci. A*, 1988, **25**, 259.
- 12 J. E. Bercaw, *J. Am. Chem. Soc.*, 1974, **96**, 5087; P. B. Hitchcock, F. M. Kerton and G. A. Lawless, *J. Am. Chem. Soc.*, 1998, **120**, 10264; M. Horáček, V. Kupfer, U. Thewalt, P. Štěpnička, M. Polášek and K. Mach, *Organometallics*, 1999, **18**, 3572.
- 13 R. D. Ernst, J. W. Freeman, P. N. Swepston and D. R. Wilson, *J. Organomet. Chem.*, 1991, **402**, 17.
- 14 R. Gleiter, personal communication.
- 15 H. P. Fritz and K.-E. Schwarzshans, *J. Organomet. Chem.*, 1964, **1**, 208; K. R. Gordon and K. D. Warren, *Inorg. Chem.*, 1978, **17**, 987.
- 16 R. D. Ernst, J.-Z. Liu and D. R. Wilson, *J. Organomet. Chem.*, 1983, **250**, 257.
- 17 L. Stahl and R. D. Ernst, *J. Am. Chem. Soc.*, 1987, **109**, 5673.
- 18 A. M. Wilson, F. G. West, A. L. Rheingold and R. D. Ernst, *Inorg. Chim. Acta*, in the press.
- 19 T. D. Newbound, A. L. Rheingold and R. D. Ernst, *Organometallics*, 1992, **11**, 1693.
- 20 J. R. Blackborow, R. H. Grubbs, K. Hildenbrand, E. A. Koerner von Gustorf, A. Miyashita and A. Scrivanti, *J. Chem. Soc., Dalton Trans.*, 1977, 2205; M. Mathew and G. Palenik, *Inorg. Chem.*, 1972, **11**, 2809; T. Dave, S. Berger, E. Bilger, H. Kaletsch, J. Pebler, J. Knecht and K. Dimroth, *Organometallics*, 1985, **4**, 1565; G. Baum and W. Massa, *Organometallics*, 1985, **4**, 1572; K. C. Sturge and M. J. Zaworotko, *J. Chem. Soc., Chem. Commun.*, 1990, 1244.
- 21 H. Schmid and M. L. Ziegler, *Chem. Ber.*, 1976, **109**, 125.
- 22 R. D. Ernst, *Struct. Bonding (Berlin)*, 1984, **57**, 1.
- 23 (a) M. Elian, M. M. L. Chen, D. M. P. Mingos and R. Hoffmann, *Inorg. Chem.*, 1976, **15**, 1148; A. Haaland, *Acc. Chem. Res.*, 1979, **12**, 415.
- 24 R. Hoffmann and P. Hofmann, *J. Am. Chem. Soc.*, 1976, **98**, 598.
- 25 R. D. Ernst and T. H. Cymbaluk, *Organometallics*, 1982, **1**, 708.
- 26 S. V. Lindeman, D. Kosynkin and J. K. Kochi, *J. Am. Chem. Soc.*, 1998, **120**, 13268; F. H. Allen, J. A. K. Howard, V. J. Hoy, G. R. Desiraju, D. S. Reddy and C. C. Wilson, *J. Am. Chem. Soc.*, 1996, **118**, 4081; M. Nishio, M. Hirota and Y. Umezawa, *The CH- $\pi$  Interaction*, Wiley-VCH, New York, 1998; H. Okawa, K. Ueda and S. Kida, *Inorg. Chem.*, 1982, **21**, 1594; K. Jitsukawa, K. Iwai, H. Masuda, H. Ogoshi and H. Einaga, *J. Chem. Soc., Dalton Trans.*, 1997, 3691.
- 27 E. Gard, A. Haaland, D. P. Novak and R. Seip, *J. Organomet. Chem.*, 1975, **88**, 181.
- 28 S. Evans, M. L. H. Green, B. Jewitt, A. F. Orchard and C. F. Pygall, *J. Chem. Soc., Faraday Trans. 2*, 1972, 1235; A. Almenningen, A. Haaland and S. Samdal, *J. Organomet. Chem.*, 1978, **149**, 219; W. Bünder and E. Weiss, *Z. Naturforsch., Teil B*, 1978, **33**, 1235; D. P. Freyberg, J. L. Robbins, K. N. Raymond and J. C. Smart, *J. Am. Chem. Soc.*, 1979, **101**, 892.
- 29 R. W. Gedridge, J. P. Hutchinson, A. L. Rheingold and R. D. Ernst, *Organometallics*, 1993, **12**, 1553; R. M. Kowaleski, F. Basolo, W. C. Trogler, R. W. Gedridge, T. D. Newbound and R. D. Ernst, *J. Am. Chem. Soc.*, 1987, **109**, 4860.
- 30 J. W. Freeman, N. C. Hallinan, A. M. Arif, R. W. Gedridge, R. D. Ernst and F. Basolo, *J. Am. Chem. Soc.*, 1991, **113**, 6509.
- 31 V. Kulsomphob, A. M. Arif and R. D. Ernst, unpublished results.
- 32 R. L. Beddoes, D. M. Spencer and M. W. Whiteley, *J. Chem. Soc., Dalton Trans.*, 1995, 2915; P. T. DiMauro and P. T. Wolczanski, *Polyhedron*, 1995, **14**, 149.
- 33 D. R. Wilson, L. Stahl and R. D. Ernst, *Organomet. Synth.*, 1986, **3**, 136.
- 34 W.-q. Weng, A. M. Arif and R. D. Ernst, *Organometallics*, 1998, **17**, 4240.
- 35 D. F. Evans, *J. Chem. Soc.*, 1959, 2003.

Paper 9/05279H